

Supplementary Materials for **Past and future drought in Mongolia**

Amy E. Hessler, Kevin J. Anchukaitis, Casey Jelsema, Benjamin Cook, Oyunsanaa Byambasuren,
Caroline Leland, Baatarbileg Nachin, Neil Pederson, Hanqin Tian, Laia Andreu Hayles

Published 14 March 2018, *Sci. Adv.* **4**, e1701832 (2018)
DOI: 10.1126/sciadv.1701832

This PDF file includes:

- fig. S1. PDSI for central Mongolia (99° to 107°E, 46° to 49°N) from observational and reanalysis data.
- fig. S2. KLP tree ring chronology used to develop the reconstruction is robust back to 49 BCE.
- fig. S3. ULP tree ring chronology used to develop the reconstruction is robust back to 488 CE.
- fig. S4. The two tree ring chronologies are both high-fidelity recorders of past drought for Mongolia.
- fig. S5. Upper and lower RMSE of the PDSI reconstruction.
- fig. S6. Quantile-quantile fits of duration and severity for pluvials and droughts.
- fig. S7. Pluvial and drought analysis using adjusted SD reconstruction.
- References (43–45)

Supplementary Materials

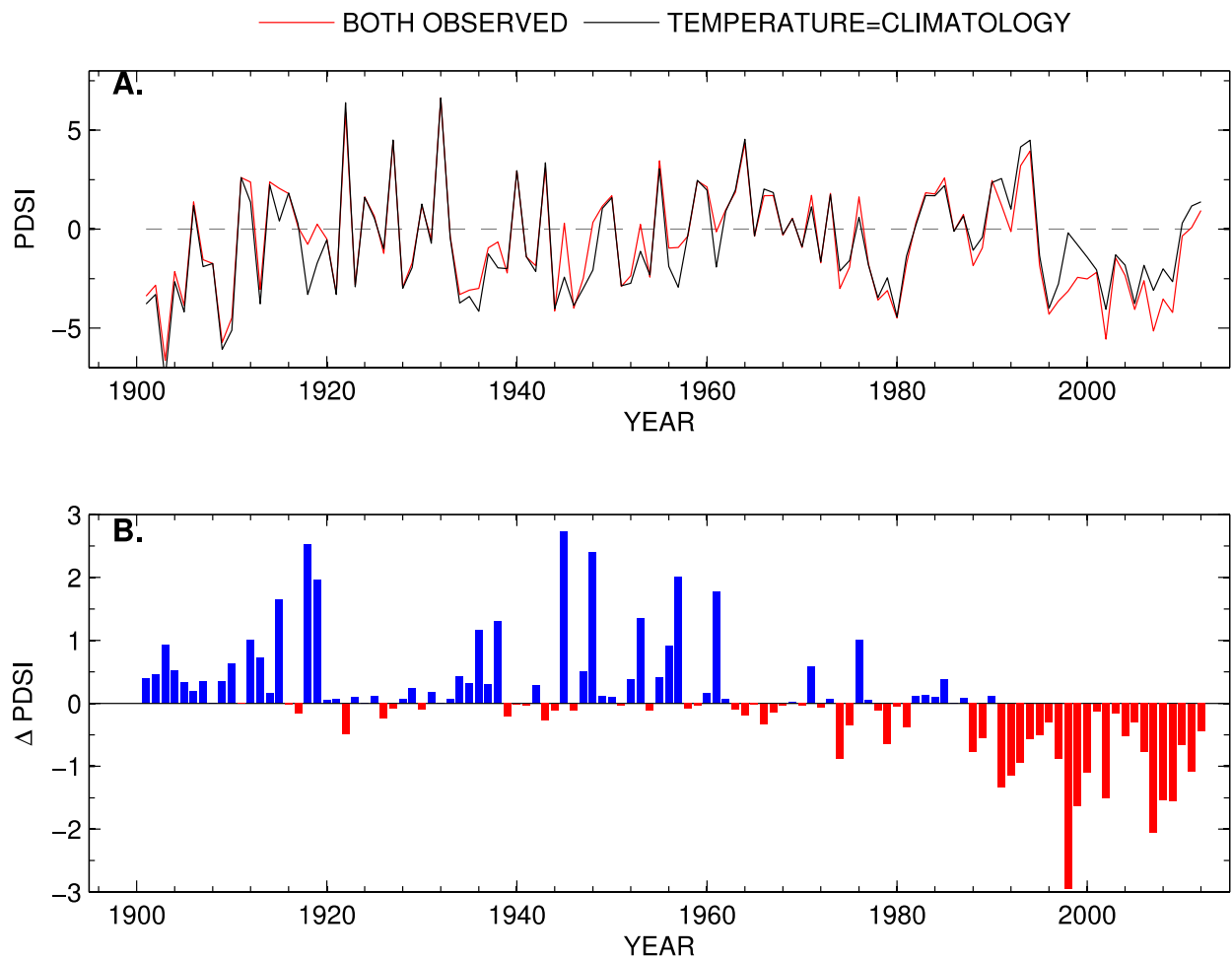


fig. S1. PDSI for central Mongolia (99° to 107°E , 46° to 49°N) from observational and reanalysis data. (A) De novo calculations of the PDSI using the Penman–Monteith method (4, 43) based on net radiation, surface pressure, and specific humidity from the 20th Century Reanalysis (44), surface temperature from the Climate Research Unity (CRU) high resolution TS3.24 gridded field (45), and precipitation from the gridded Global Precipitation Climatology Centre (GPCC) data[4]. The Penman–Monteith PDSI was calculated twice: once with all the climate data ('BOTH OBSERVED') and again with the transient temperature replaced by the long-term monthly climatology. Panel (B) shows the difference between the two PDSI calculations.

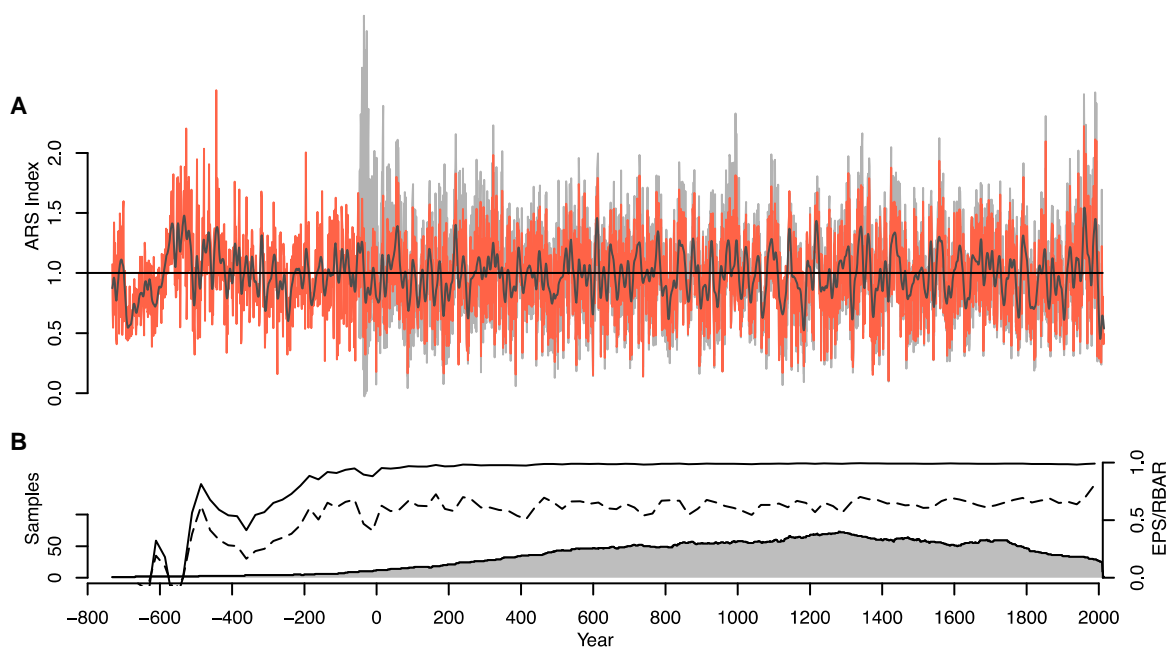


fig. S2. KLP tree ring chronology used to develop the reconstruction is robust back to 49 BCE. (A) Detrended tree-ring chronology (red) with bootstrapped 95% confidence limits around the mean (grey), 15-yr smoothing spline (black) and (B) sample depth (grey polygon), running EPS (expressed population signal) (black), and rbar (dashed line) for *Pinus sibirica* chronology from Khorgo (KLP).

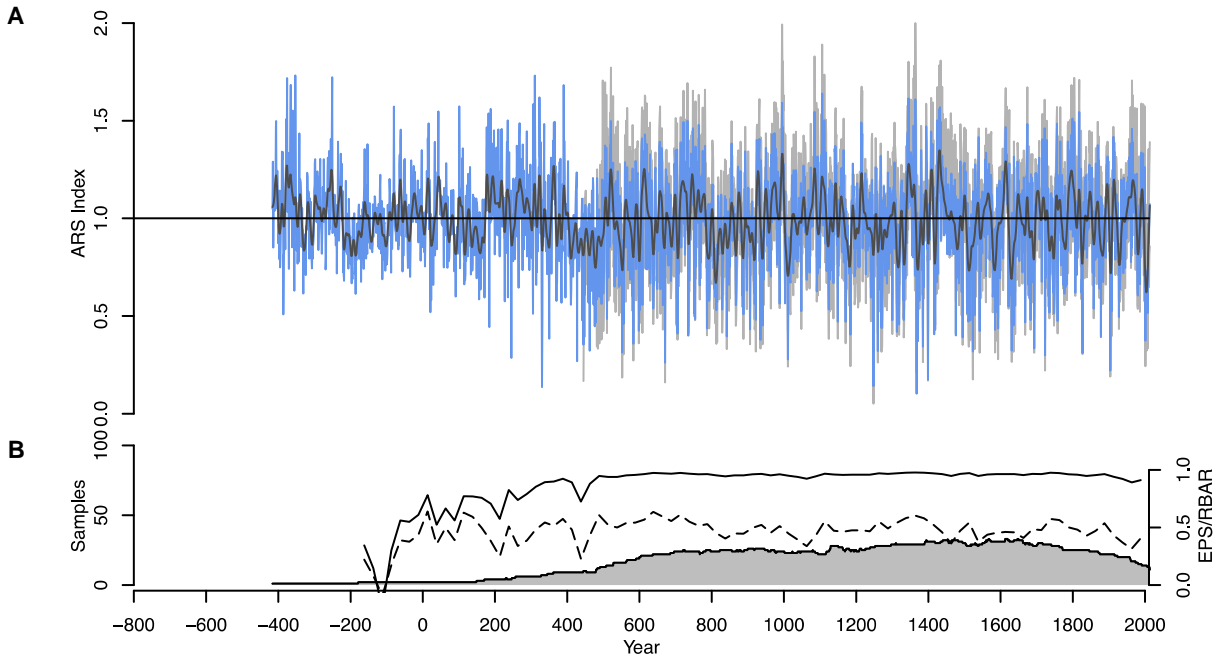


fig. S3. ULP tree ring chronology used to develop the reconstruction is robust back to 488 CE. (A) Detrended tree ring chronology (red) with bootstrapped 95% confidence limits around the mean (grey), and 15-yr smoothing spline (black) and (B) sample depth (grey polygon), running EPS (expressed population signal) (black), and rbar (dashed line) for *Pinus sibirica* chronology from Uurgat (ULP).

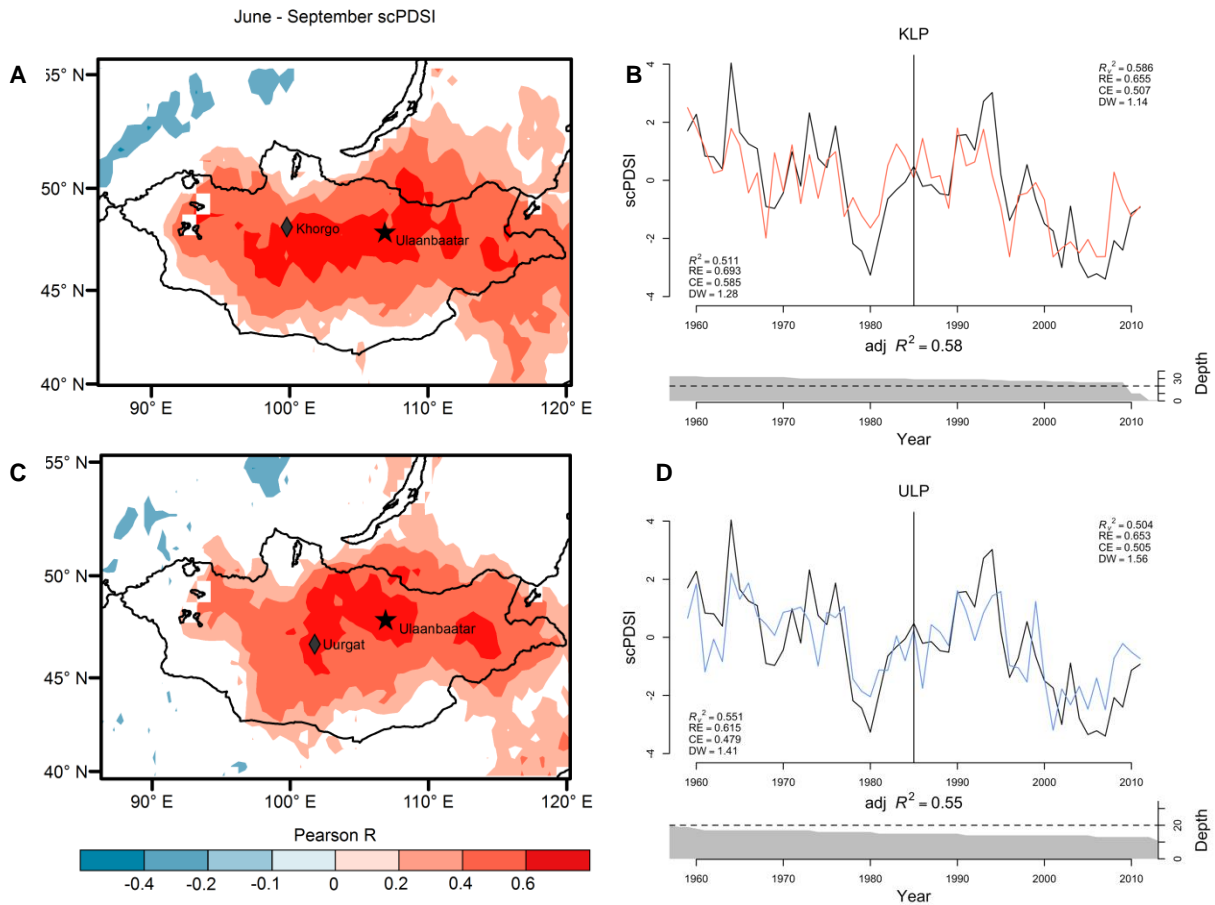


fig. S4. The two tree ring chronologies are both high-fidelity recorders of past drought for Mongolia. (A) Correlation between the mean of Khorgo (KLP) and (C), Urgat (ULP) *Pinus sibirica* tree ring chronologies (diamonds) and gridded CRU 3.21 PDSI (24). (B, D), Calibration plots of CRU 3.21 PDSI (black) for a grid box over north central Mongolia (46–49 N, 99–109 E) and the mean of the tree ring chronologies (Khorgo - red and Urgat - blue). Calibration and verification statistics for the early (1959–1985) and late (1986–2011) portions of the split calibration/verification period (vertical line) include verification R^2 (R_v^2), reduction of error (RE), coefficient of efficiency (CE) and Durbin-Watson statistic (DW). Overall R^2 for entire calibration period is also noted (adj R^2).

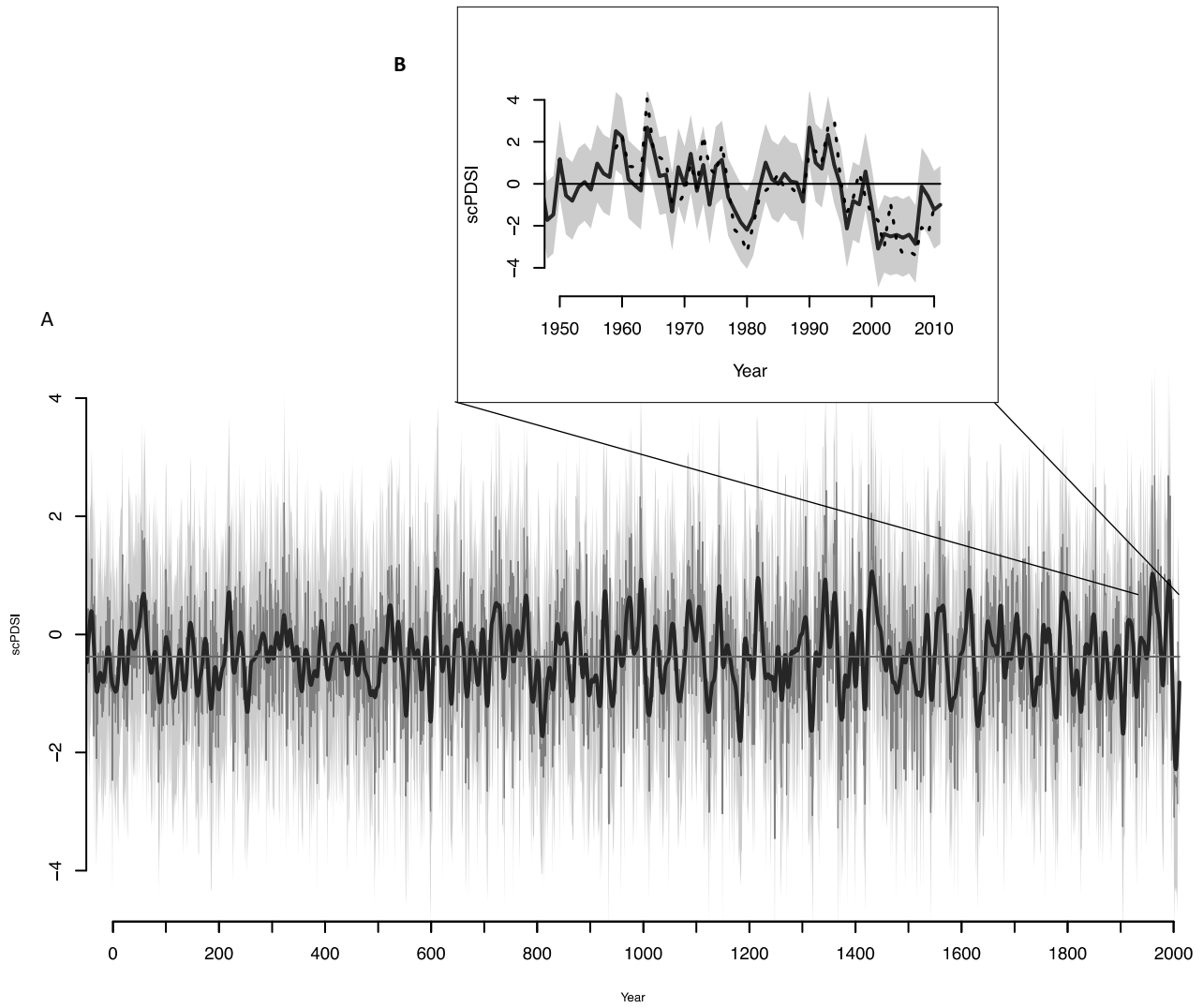


fig. S5. Upper and lower RMSE of the PDSI reconstruction. (A) Upper and lower RMSE (light grey) and 15-year spline (black) of the PDSI reconstruction (dark grey) (B) with an inset of the 1950-2011 period including the instrumental target PDSI (dotted line).

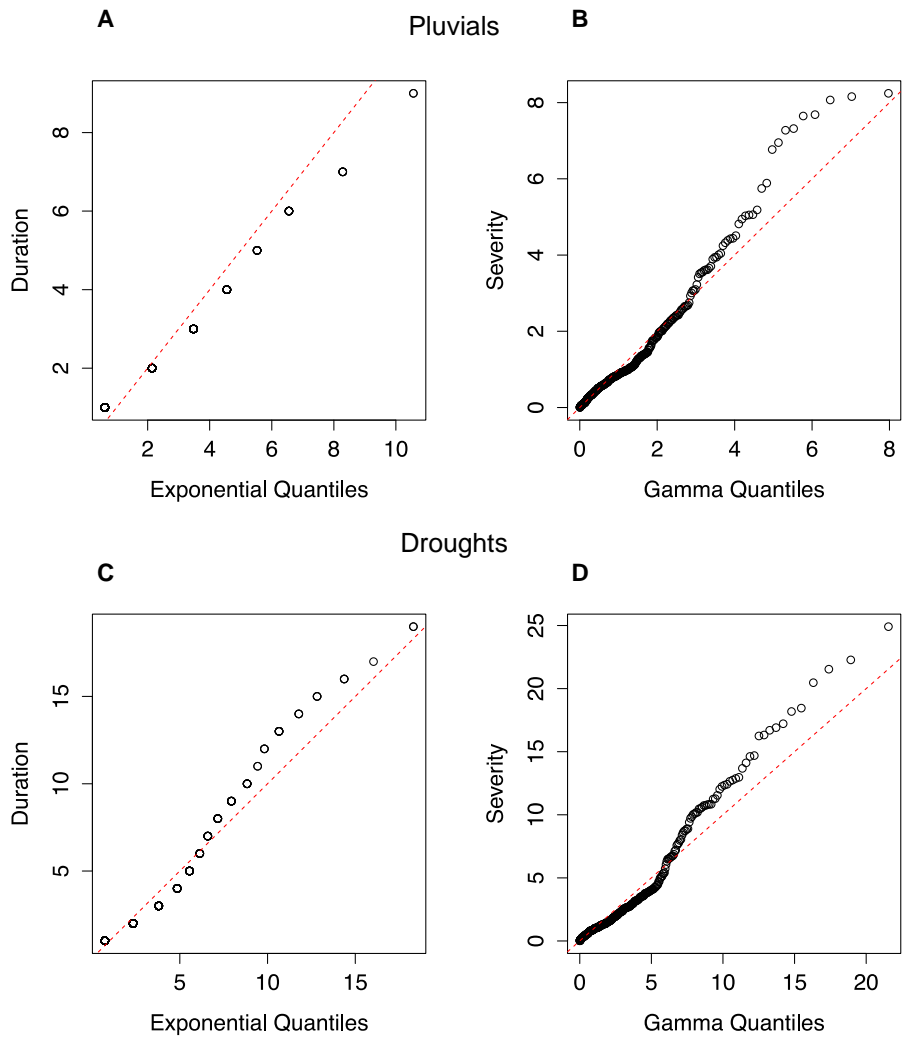
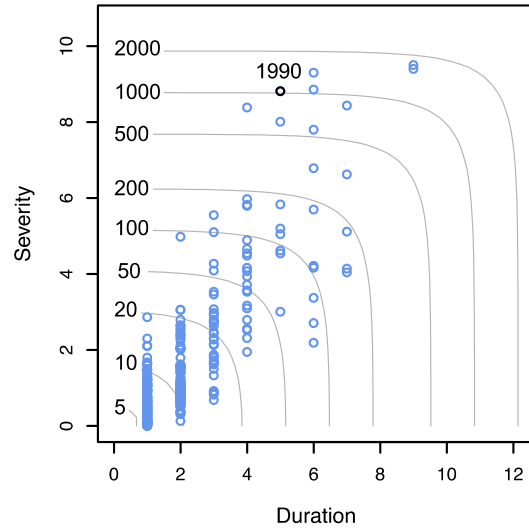


fig. S6. Quantile-quantile fits of duration and severity for pluvials and droughts. Quantile-quantile plots of pluvial (A), duration and (B), severity and drought (C), duration and (D), severity. Duration was modeled with an exponential distribution, and severity with a gamma distribution. These figures indicate that the selected distributions are somewhat lighter-tailed (less prone to extreme values) than the data which they model, but are reasonable fits of duration (A), and severity (B), with one-to-one line (red dash).

B



B

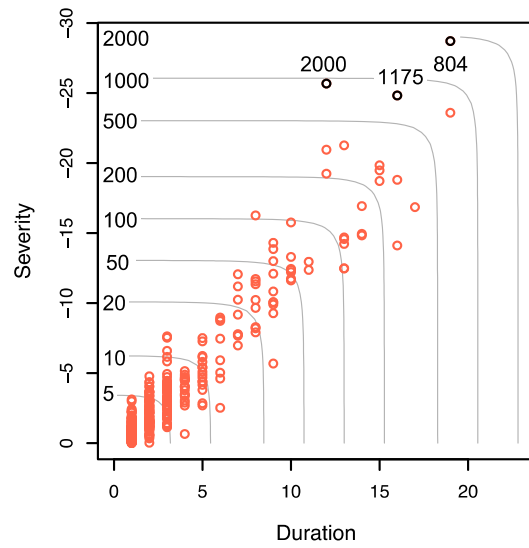


fig. S7. Pluvial and drought analysis using adjusted SD reconstruction. Pluvial (A) and drought (B) duration, severity and return time (contours) using reconstruction with SD adjusted to the instrumental SD during the calibration period (1959-2011). Duration and return time of extreme pluvials and droughts does not change but the severity gets more extreme due to the increase in the SD. Highlighted pluvial (1990) and droughts (804, 1175, and 2000) in black.